NON-DESTRUCTIVE HEALTH MONITORING BY CRACK IDENTIFICATION FOR SIMPLY SUPPORTED FIBER REINFORCED COMPOSITE STRUCTURES

Mohamed S. Gaith, mgaith@coe.neu.edu Department of Mechanical Engineering, Al Balqa Applied University, Amman, Jordan

Ahmad Zaben, Naeem Bawayah, Yazan Israwi, Mosa'ab Farraj, Department of Mechanical Engineering, Al Balqa Applied University, Amman, Jordan

ABSTRACT

A crack in structural member introduces local flexibility which is function of crack depth. This flexibility changes the dynamic behavior of the system and its stability characteristics. A continuous cracked beam vibration theory is implemented for the lateral vibration of cracked Euler–Bernoulli beams with single-edge open cracks. In this work, the crack identification (health monitoring) for simply supported graphite/epoxy fiber reinforced composite beams is considered. The effects of crack depth and height, fiber orientation, and fiber volume fraction on the flexibility and consequently on natural frequency and mode shapes for cracked fiber reinforced composite beams are investigated.

Keywords: crack, fiber reinforced composite structure, local flexibilty, natural frequency.

1. INTRODUCTION

The proper selection of the orientation angle of the different layers of fiber is a key feature in the design of composite structures. In fiber composites, the stiffness of the individual plies depends on the angles of fiber orientation with respect to the loads. High speed machinery and lightweight structures require high strength-to-weight ratios. For this reason, in recent years, the use of anisotropic reinforced composites, for which strength-to-weight ratios are very high, has increased substantially in the fields of mechanical and civil engineering [Vinson and Chou, 1975]. Cracks occurring in structural elements are responsible for local stiffness variations [Irwin, 1956], which in consequence affect their dynamic characteristics, namely, natural frequency and damping. [Cawley and Adams, 1979] detected damage in composite structures by frequency variation. [Karaagac et al, 2009] studied the cracked beam using finite element analysis and compared with experimental results. [Krawczuk and Ostachowicz, 1995] studied the effects of crack on Euler Bernoulli cantilever composite beam using the local compliance matrix [Nikpour and Dimarogonas, 1988] for unidirectional composite materials. Using the local flexibility concept, [Song et al, 2003] studied the same problem using Timoshenko beam theory. The cracked beam is modeled as two segments interconnected by a mass less rotational spring. In the present study a model of a fiber reinforced composite simply supported beam with a transverse one-edge non-propagating open crack is considered. By using this model, the influence of the depth and location of the crack, ply orientation angle, and fraction of fibers on the bending natural frequencies of the simply supported composite beam have been investigated.

2. Cracked Composite Beam Model:

The vibration of a fiber reinforced composite simply supported beam with edge transverse surface crack is considered. The crack in structural member introduces local flexibility as a mass less rotational spring and is function of crack depth. This flexibility changes the dynamic behavior of the system and its stability characteristics. The vibration theory, linear fracture mechanics, the Castigliano theory and lamination theory are used to model the cracked beam system as Euler Bernoulli beam. The cracked beam is modeled as two segment interconnected by a rotational spring. Eight boundary conditions were obtained used to solve the Euler-Bernoulli beam equation for the two segments as depicted in Fig. 1. The additional elastic deformation energy U of the composite beam due to the crack can be expressed, in general form, by the relation [Nikpour and Dimarogonas, 1988]

$$U = \int_A (D_1 \sum_{i=1}^{i=N} K_{Ii}^2 + D_2 \sum_{i=1}^{i=N} K_{Ii} + D_3 \sum_{i=1}^{i=N} K_{IIi}^2 + D_4 \sum_{i=1}^{i=N} K_{IIIi}^2) dA \qquad (1)$$

where K_{Ii} , K_{IIi} and K_{IIIi} are the stress intensity factors corresponding to three modes of the crack. The coefficients D_1 , D_2, D_3, and D_4, given by [Nikpour and Dimarogonas, 1988] as:

$$D_1 = -0.5\bar{b}_{22}\,\mathrm{Im}\left(\frac{s_1+s_2}{s_1 s_2}\right)$$

$$D_2 = \bar{b}_{11}\,\mathrm{Im}(s_1 s_2) \qquad (2)$$

$$D_3 = 0.5\bar{b}_{11}\,\mathrm{Im}\left(\frac{s_1+s_2}{s_1 s_2}\right), \quad D_4 = \frac{1}{2}\sqrt{b_{44} b_{55}}$$

The complex constants s_1 and s_2 are roots of the characteristic equation [Sih and Chen, 1981]:

$$\bar{b}_{11} s^4 - 2\bar{b}_{16} s^3 + (2\bar{b}_{12} + \bar{b}_{66}) s^2 - 2\bar{b}_{26} s + \bar{b}_{22} = 0 \qquad (3)$$

The constants $\bar{b}_{ij}$ are calculated from the relations [Sih and Chen, 1981]:

$$\begin{aligned}
\bar{b}_{11} &= b_{11} m^4 + (2b_{12} + b_{66}) m^2 n^2 + b_{22} n^4 \\
\bar{b}_{22} &= b_{11} n^4 + (2b_{12} + b_{66}) m^2 n^2 + b_{22} m^4 \\
\bar{b}_{12} &= (b_{11} + b_{22} - b_{66}) m^2 n^2 + b_{12}(m^4 + n^4) \\
\bar{b}_{16} &= (-2b_{11} + 2b_{12} + b_{66}) m^3 n + (2b_{22} - 2b_{12} - b_{66}) m n^3 \\
\bar{b}_{26} &= (-2b_{11} + 2b_{12} + b_{66}) n^3 m + (b_{22} - 2b_{12} - b_{66}) n m^3 \\
\bar{b}_{66} &= 2(2b_{11} - 4b_{12} + 2b_{22} - b_{66}) m^2 n^2 + b_{66}(m^4 + n^4)
\end{aligned} \qquad (4)$$

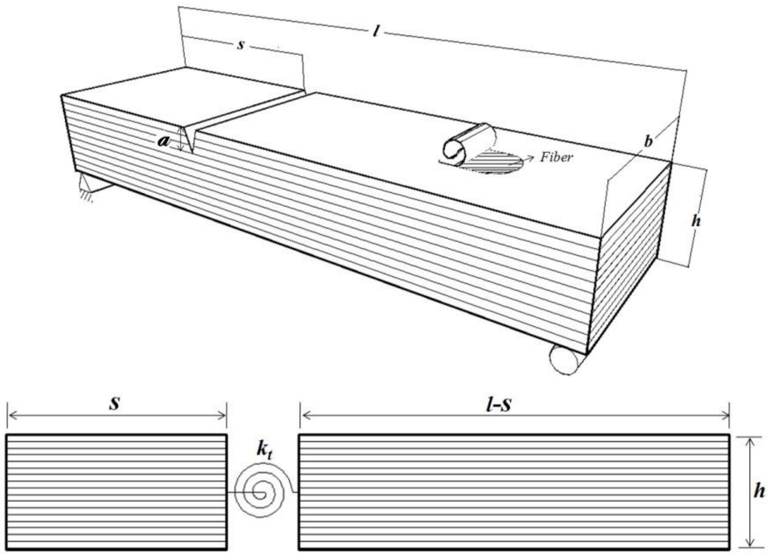

Figure 1 The geometry and model of unidirectional fiber reinforced composite simply supported beam with transverse open crack.

Where m=cos α and n=sin α (α denotes the orientation angle). The terms b_{ij} are related to the mechanical constants of the material.

$$b_{11} = \frac{1}{E_{11}}(1 - \nu_{12}^{\ 2}\frac{E_{22}}{E_{11}})$$
$$b_{22} = \frac{-\nu_{12}}{E_{11}}(1 + \nu_{23}) \qquad (5)$$
$$b_{66} = \frac{1}{G_{12}} \qquad b_{44} = \frac{1}{G_{23}} \qquad b_{55} = b_{66}$$

whereas the mechanical properties of the composite E_{11}, E_{22}, G_{12}, υ_{12} and ρ are calculated by using the following formulas [Vinson and Sierakowski, 1991], the subscript f denotes fiber, the subscript m denotes matrix and E, G, υ and ρ are the modulus of elasticity, the modulus of rigidity, the Poisson's ratio and the mass density, respectively):

$$\rho = \rho_f V + \rho_m (1 - V)$$
$$E_{11} = E_f V + E_m (1 - V)$$
$$E_{22} = E_m \left[\frac{E_f + E_m + (E_f - E_m)V}{E_f + E_m - (E_f - E_m)V} \right]$$
$$\nu_{12} = \nu_f V + \nu_m (1 - V) \qquad (6)$$
$$\nu_{23} = \nu_f V + \nu_m (1 - V) \left[\frac{1 + \nu_m + \nu_{12} E_m / E_{11}}{1 - \nu_m^{\ 2} + \nu_m \nu_{12} E_m / E_{11}} \right]$$
$$G_{12} = G_m \left[\frac{G_f + G_m + (G_f - G_m)V}{G_f + G_m - (G_f - G_m)V} \right]$$

Generally, for anisotropic materials, the stress intensity factors K_{ij} (j=I, II, III; i =1,N) for the crack in the composite beam according to [Bao et al, 1992] can be written as:

$$K_{ji} = \sigma_i \sqrt{\pi a} \mathrm{F}_{ji} \left(a/h, \lambda^{1/4} l/h, \zeta \right) \tag{7}$$

where σ_i denotes the stress at the crack cross section due to the i_{th} independent force acting on the beam, a is the depth of the crack, F_{ji} denotes the correction function (j=I, II, III; i =1,N), λ and ζ are dimensionless parameters which characterize the in-plane orthotropy and l and h are the length and height of the beam, respectively, as shown in Fig. 1.

The dimensionless parameters λ and ζ are defined as functions of the elastic constants by [Suo, 1990]

$$\lambda = E_{22} / E_{11} \quad , \quad \zeta = \sqrt{E_{11} E_{22}} / 2G_{12} - \sqrt{\nu_{12} \nu_{21}})$$

It was shown by [Bao et al, 1992] that the effect of $\lambda^{1/4} l/h$ is negligible. Hence:

$$K_{ji} = \sigma_i \sqrt{\pi a} \mathrm{Y}_j (\zeta) F_{ji} \left(a/h \right) \tag{8}$$

Where Y_j is the correction function which takes into account anisotropy of the material. And $F_{ji}\left(a/h \right)$ is the correction function which takes into account finite dimensions of the beam. With account taken of the fact that the beam analyzed is subjected only to the bending moment, the additional elastic deformation energy is [Crawczuk et al, 1995]

$$\mathrm{U} = D_1 \int_A K_{IS}^2 dA \quad , \tag{9}$$

Where K_{IS}^2 is the stress intensity factor corresponding to the bending moment $M_{\circ}$ acting on the beam with

$$K_{IS}^2 = (6M_o / bh^2) \sqrt{\pi a} Y_1(\zeta) F_{IS}(a/h) \tag{10}$$

The correction functions $Y_1(\zeta)$ and $F_{IS}(a/h)$ are given as:

$$Y_1 = 1 + 0.1(\zeta - 1) - 0.016(\zeta - 1)^2 + 0.002(\zeta - 1)^3 \tag{11}$$

$$F_{IS}(a/h) = \sqrt{\tan\gamma / \gamma} \left[0.923 + \frac{0.199(1 - \sin\gamma)^4}{\cos\gamma} \right] \tag{12}$$

Where $\gamma = \pi a / 2h$

Following the same procedure used by [Crawczuk, 1995] by applying the Castigliano theorem, part II, [Przemieniecki, 1967] yields the additional flexibility C_{55}^1 of the composite beam due to the transverse one edge open crack as

$$C_{55}^{1} = \frac{72D_1\pi}{bh^2}\int_0^{\bar{a}}\left[\bar{a}Y_I(\zeta)^2F_{I5}(\bar{a})^2\right]d\bar{a} \tag{13}$$

Where $\bar{a} = a/h$ and $d\bar{a} = da/h$

The additional flexibility of the beam due to the crack can be presented in non-dimensional form as:

$$p = IS_{11}c_{55}^{1}/L \tag{14}$$

Where I is the geometrical moment of inertia of the beam cross-section and S_{11} is given as

$$S_{11} = \bar{S}_{11}m^4 + 2(\bar{S}_{12} + 2\bar{S}_{33})m^2n^2 + \bar{S}_{22}n^4 \tag{15}$$

The terms S_{ij} are determined from the relations [Vinson and Sierakowski, 1991]:

$$S_{11} = \frac{E_{11}}{(1 - V_{12}^{2}E_{22}/E_{11})} \quad , \bar{S}_{22} = \bar{S}_{11}E_{22}/E_{11} \quad , \bar{S}_{12} = v_{12}S_{22} \quad , \bar{S}_{33} = G_{12}$$

Substituting Eq.13 into Eq .14 yields:

$$p = 6D_1S_{11}\pi\frac{h}{l}\int_0^{\bar{a}}\left[\bar{a}Y_I(\zeta)F_{I5}(\bar{a})\right]d\bar{a} \tag{16}$$

For the fiber reinforced composite beam, due to the crack existence, the local flexibility appears and can be derived as shown in Eq. 16

Flexibility variation due to the change in fiber volume fractions (V_f) and crack depths (a) at constant orientation angle ($\theta = 0$) is shown in Fig. 2 with l=1m, h=0.025m, b=0.05m and material properties for graphite/epoxy fiber reinforced composite simply supported beam listed in Table 1.

Table 1 The material properties for the composite beam.

	$E\,(GPa)$	$G\,(GPa)$	$\rho\,(Kg/m^3)$
Fiber	275.6	114.8	1900
Matrix	2.756	1.03	1600

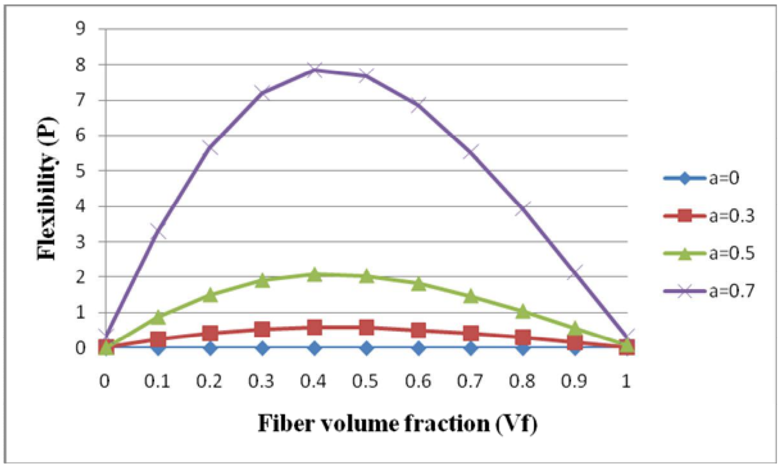

Figure 2 Flexibility changes with fiber volume fraction with θ= 0, a = 0, 0.3, 0.5, 0.7.

Figure 2 shows the effect of fiber volume fraction (V_f) on the flexibility for different crack depth a = 0.0, 0.3, 0.5 and 0.7. For V_f = 0 and *1*, the flexibility magnitude is diminished .This occurs because at these both values, the material will be eventually isotropic material. When $0 < V_f < 1$, the anisotropy of the material appears and the flexibility appears too .The flexibility increases as V_f increases up to 0.4, then decreases to vanish at V_f = 1. On the other hand, by increasing the crack depth, the flexibility magnitude increases (or the stiffness magnitude of the beam decreases). It is significant to mention that the maximum flexibility magnitude reached when (V_f = 0.4) for all crack depths.

Flexibility variation due to the change in fiber volume fractions (V_f) and crack depths a at constant orientation angle($\theta = 90$) is shown in Fig. 3. A reverse behavior shown in Fig. 3, the flexibility is maximum at V_f = 0 and 1, representing isotropic material. The flexibility is decreasing by increasing V_f up to 0.4 then the flexibility is increasing till V_f = 1.0 .The flexibility magnitude is much smaller for $\theta = 90$ than that for $\theta = 0$. This implies that flexibility is effective when fibers are perpendicular to the crack width.

Figure 4 represents flexibility changes with changing in fiber orientation angle at different crack depths with constant fiber volume fraction (V_f =0.5). The figure shows the effect of fiber orientation on the flexibility when $\theta = 0$, fibers are perpendicular to crack width, the flexibility (stiffness reduction) is maximum. As the fiber inclines in direction to the direction of crack width, the flexibility effect decreases to vanish when the fiber direction is parallel to crack depth, $\theta = 90$. The larger the crack depth is, the larger the flexibility is. It is clearly shown that the flexibility due to the crack in the composite beam is a function of the anisotropy of material, the volume fraction of fibers, the angle between the fibers and the crack and the crack depth.

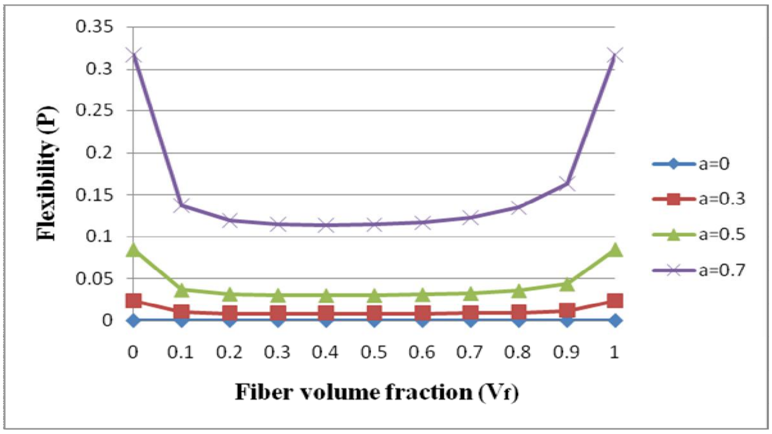

Figure 3 Flexibility changes with fiber volume fraction with $\theta = 90$, $a = 0, 0.3, 0.5, 0.7$.

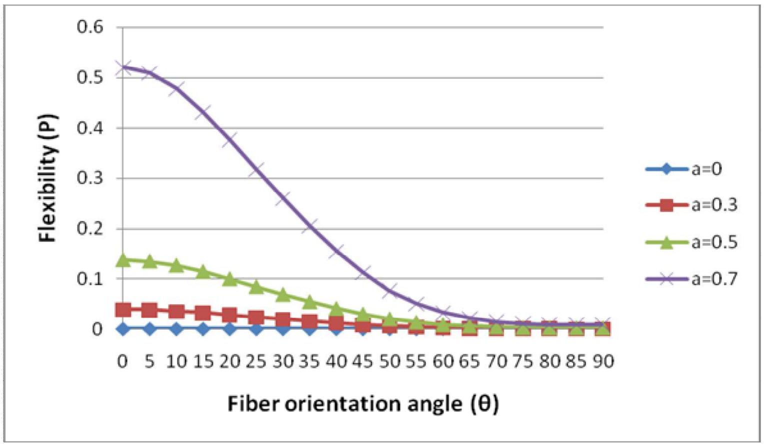

Figure 4 Flexibility changes with fiber volume fraction at crack depths ($a = 0, 0.3, 0.5, 0.7$)

3 RESULTS AND DISCUSSION

3.1 Natural Frequencies for Composite Beams

In this section the natural frequencies for simply supported fiber reinforced composite beam is presented. The material properties and dimensions are chosen same as in previous section since they are widely used in many engineering applications like aircrafts, wind turbines, formula cars, etc. The first two natural frequencies for simply supported composite beam with eight plies stacking with $[90]_{4s}$, $[0]_{4s}$ and $[45]_{4s}$ are presented in Figs. 5, and 6, respectively, as function of fiber volume fraction (V_f). From these figures, the natural frequencies are increasing by increasing the fiber volume fraction (V_f).This is expected since the material properties for fibers are of large values. The orientation angle θ has significant effect on the natural frequency as shown in the Figs. 5-6. The natural frequencies of zero fiber orientation angle $\theta = 0$ are higher than that for those angles ($\theta = 45$) and ($\theta = 90$), thus with increasing in the fiber orientation angle there is a corresponding decreasing in natural frequencies with volume fiber fraction increment. It is noted that at zero fiber volume fraction (100% matrix) and at unity of fiber volume fraction (100% fiber) all three types of natural frequencies have the same values for the case of 0 and 1 fiber volume fraction. This corresponds to the isotropic material where the orientation angle is not affecting the natural frequencies.

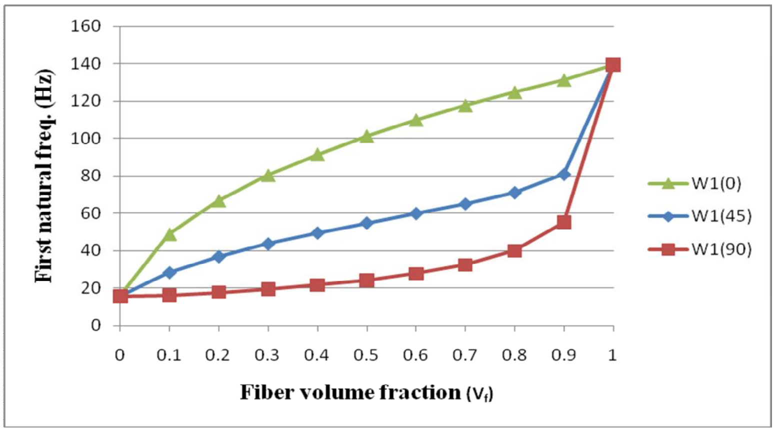

Figure 5 The relation between the first natural frequencies and fiber volume fraction for simply supported beam fiber orientation angles (θ = 0, 45, and 90)

3.2 The Effects of Crack Depth and Location on the Natural Frequencies:

From Fig.7, when V_f = 0.5, a = 0.2, 0.3, 0.5, 0.7 and 0.8 with non dimensional crack locations (s) from 0 to 1 for simply supported composite beam, the first natural frequency is maximum at crack location (s = 0) and (s = 1), which corresponds to the uncracked beam. The natural frequency decreases from crack location (s = 0) till the minimum value at crack location (s = 0.5), then increase to the maximum value at crack location (s = 1). For the second natural frequency as shown in Fig. 8 is maximum at crack locations (s = 0), (s = 0.5) and (s=1), and minimum at crack locations (s = 0.2) and (s = 0.8). The natural frequency decreases from crack location (s) of zero till the minimum value at crack location (s = 0.2), then increases to maximum value at crack location (s = 0.5). The curve is symmetric around the middle crack position (s = 0.5). As the crack depth increases, the corresponding natural frequencies decrease for each crack location. This is compatible with the increase of flexibility, or decrease in the stiffness of the beam. Similar trend can be found in Figs 9 and 10 for θ = 90.

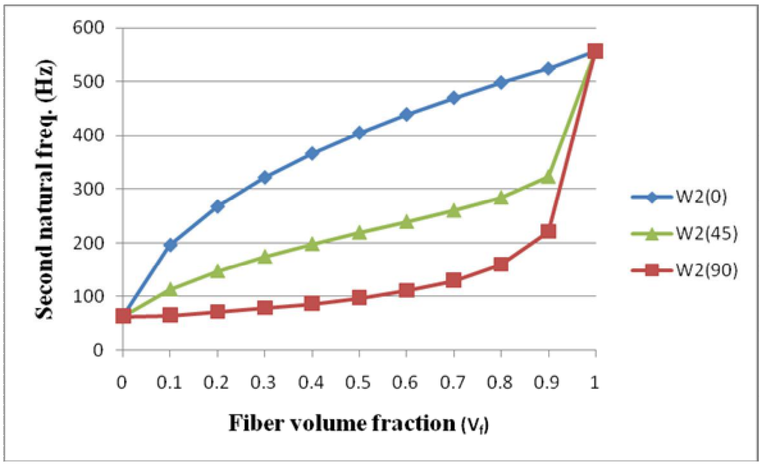

Figure 6 The relation between the second natural frequencies and fiber volume fraction for simply supported beam fiber orientation angles (θ = 0, 45, and 90)

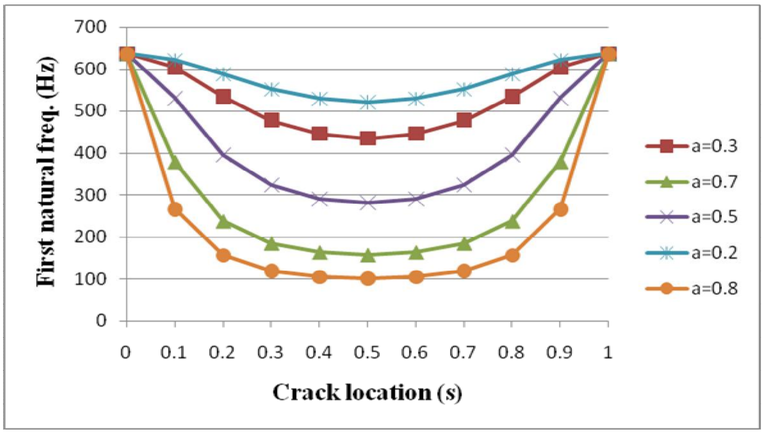

Figure 7 The relation between the first natural frequencies and non dimensional crack locations for simply supported composite beam with (a = 0.2, 0.3, 0.5, 0.7 and 0.8), V_f = 0.5, $\theta = 0$

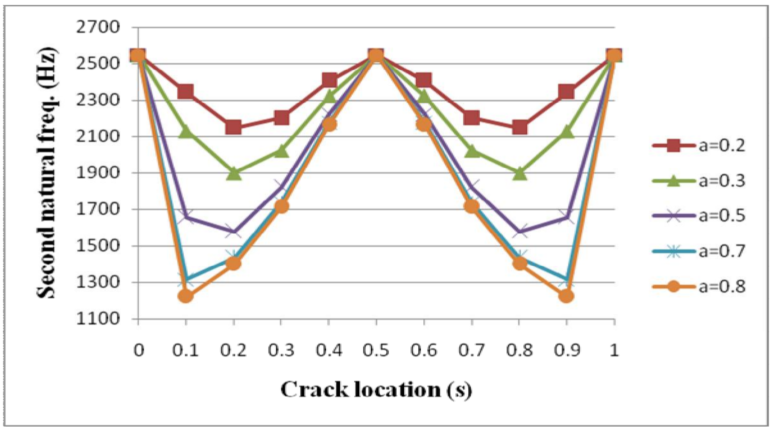

Figure 8 The relation between the second natural frequencies and non dimensional crack locations for simply supported composite beam with (a = 0.2, 0.3, 0.5, 0.7 and 0.8), V_f = 0.5, $\theta = 0$

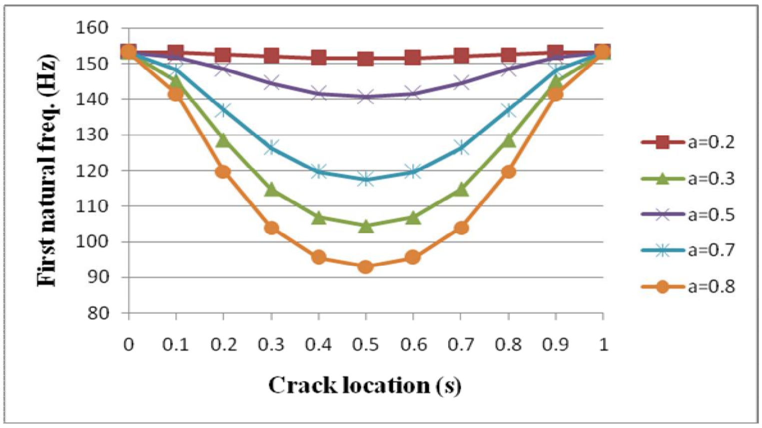

Figure 9 The relation between the first natural frequencies and non dimensional crack locations for simply supported composite beam with (a = 0.2, 0.3, 0.5, 0.7 and 0.8), V_f = 0.5, θ = 90

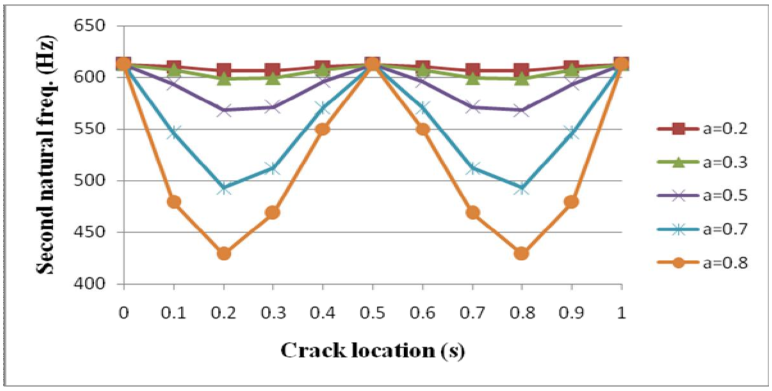

Figure 10 The relation between the second natural frequencies and non dimensional crack locations for simply supported composite beam with (a = 0.2, 0.3, 0.5, 0.7 and 0.8), V_f = 0.5, θ = 90

Next, by varying crack depth at constant non dimensional crack location, the first and second natural frequencies are calculated for V_f = 0.5, θ = 0 and 90, as shown in Figs. 11 and 12, respectively. It's shown from these figures that the natural frequency at fiber orientation angle (θ = 0) is higher than that at (θ = 90), and this is due to the flexibility which will be higher in the case of (θ = 90). It's clear that the natural frequency will decrease with increasing in the crack depth.

3.3 Mode Shapes for Fiber Reinforced Composite Beams

In the previous sections, the mathematical modeling representing the vibration motion of the fiber reinforced composite was investigated and the natural frequencies of the system were calculated. In this section, the corresponding mode shapes for cracked composite simply supported beam will be presented for different crack locations and depths.

Figures 13 and 14 show the first mode shape at crack location (s = 0.1) with V_f = 0.5 for crack depth (a = 0.3 and 0.7), respectively. From these figures, the existence of crack will change the stiffness of

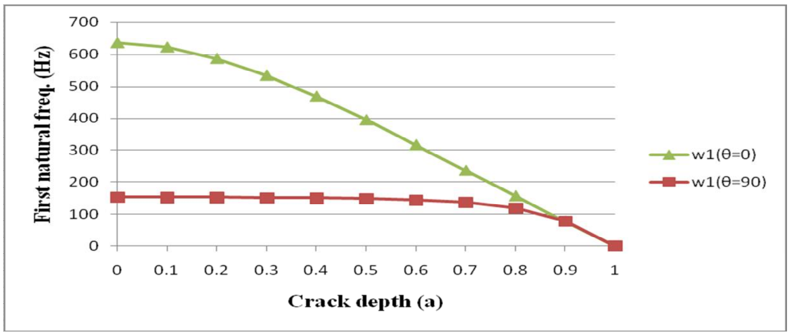

Figure 11 The relation between first natural frequency and non dimensional crack depth for simply supported composite beam at fiber orientation angles (θ = 0 and 90), s = 0.2 and V_f = 0.5.

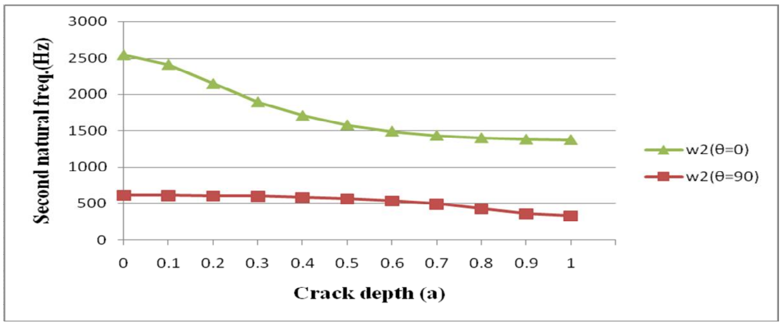

Figure 12 The relation between second natural frequency and crack depth for simply supported composite beam at fiber orientation angles (θ = 0 and 90), s = 0.2 and V_f = 0.5.

the beam, and this can be noted from shifting the mode shape from healthy mode to the left. The larger the crack depth is, the larger the deviation that the mode shape experiences. The mode shape is shifted to left since crack depth located at the left side, (s = 0.1).

Figures 15 and 16 present the second mode shapes for cracked simply supported eight plies $[0]_{4s}$ composite beam with crack location at (s = 0.1) for a = 0.3 and 0.7, respectively. The existence of crack will change the stiffness of the beam, and this can be noted from the shifting of healthy mode to the left. It can be noted that the nodal point for the second mode is shifted to left from the original theoretical uncracked beam (which is located at s = 0.5), while it is found at (s = 0.45 and 0.46) for a = 0.3 and 0.7, respectively. The deterioration of mode shape is significant for (a = 0.7).

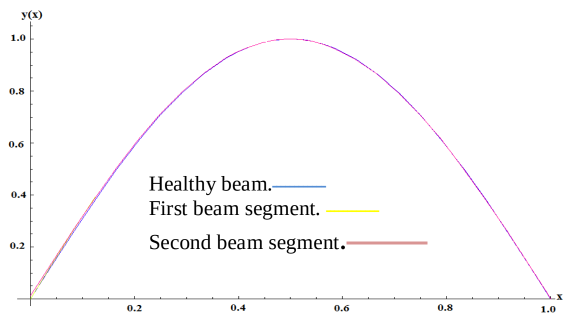

Figure 13 First mode shape for cracked simply supported beam when (s = 0.1, a = 0.3, θ = 0).

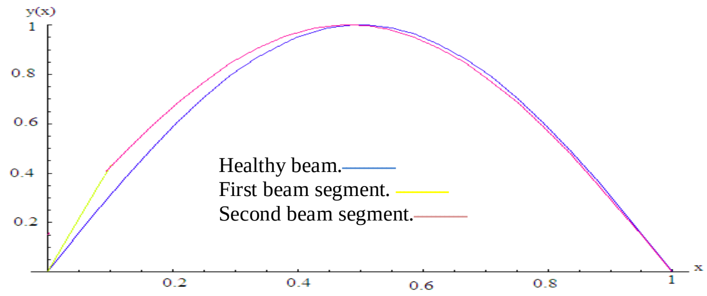

Figure 14 First mode shape for cracked simply supported beam when (s = 0.1, a = 0.7, θ = 0).

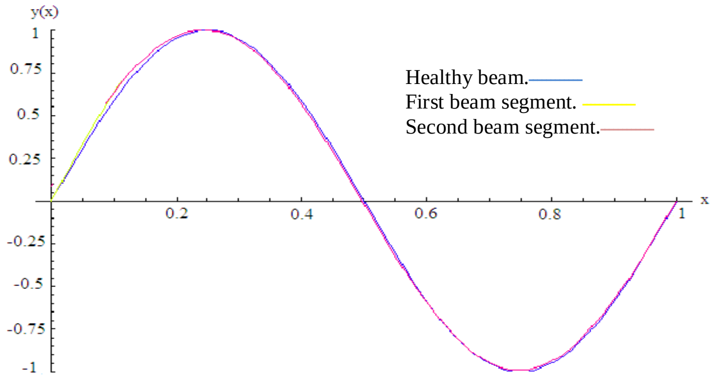

Figure 15 Second mode shape for cracked simply supported beam (s = 0.1, a = 0.3, θ = 0).

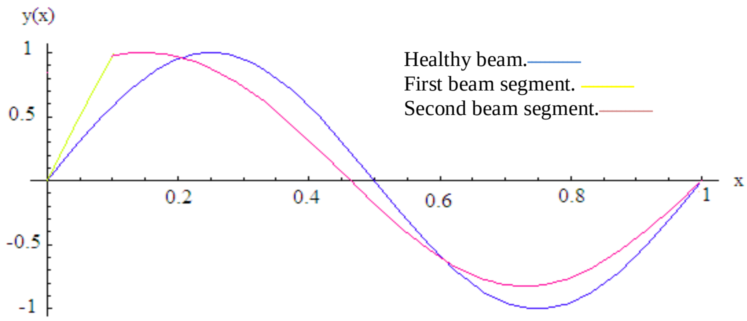

Figure 16 Second mode shape for cracked simply supported beam when (s = 0.1, a = 0.7, θ = 0).

4. CONCLUSIONS

The crack identification for fiber reinforced composite simply supported beams is investigated. In modeling and analyzing the system, theory of fracture mechanics, theory of elasticity, theory of composite lamination, and theory of vibration were implemented to obtain the two main parameters, namely, natural frequency and corresponding mode shapes to identify (or on line health monitoring) cracked composite beams. The cracked beam is modeled as two segment interconnected by rotational spring. Eight boundary conditions were used to solve the Euler-Bernoulli beam equation for the two segments. The effects of crack depth and crack location, anisotropic properties such as angle orientation and fiber volume fraction on the flexibility and natural frequency for fiber reinforced composite beam are revealed. For composite simply supported beam, at constant crack location, the first and second natural frequencies are found to decrease as the crack depth increases. The first natural frequency is decreasing as the crack location is going away from the support till the minimum value at the mid span. This is due to the fact the bending stress is maximum at that location. The mode shape for simply supported beam is deteriorated upon the existence of the crack, and this deterioration is increasing as the crack depth increases. The mode shape shifts to the side where the crack is located. The nodal point for the second mode is varying depending on the crack depth and location. The variation of natural frequencies and mode shape may be used to detect the crack profile for on-line structural health monitoring.

5. REFERENCES

1. **Cawley, P., Adams, R.D., (1979)**, "A Vibration Technique for Non-Destructive Testing of Fiber Composite Structures", Journal of Composite Materials 13, 161-175.

2. **Bao, G., Ho, S., Suo, Z. and Fan, B., (1992)**, " The Role of Material Orthotropy in Fracture Specimens for Composites", Journal of Solids and Structures 29, 1105-1116.

3.**Karaagac, C., Öztürk, H., and Sabuncu, M., (2009)**, " Free vibration and lateral buckling of a cantilever slender beam with an edge crack: Experimental and numerical studies", Journal of Sound and Vibration 326, 235-250.

4. **Krawczuk, M., Ostachowicz, W. M., (1995)**, "Modeling and Vibration Analysis of a Cantilever Composite Beam with a Transverse Open Crack", Journal of Sound and Vibration 183(1), 69-89.

5. **Nikpour, K., and Dimarogonas, A. D., (1988)**, "Local compliance of Composite Crack Bodies", Journal of Composite Science and Technology 32, 209-223.

6. **Sih, G. C., and Chen, E. P., (1981)**, Cracks in Composite Materials. London: Martinus Nijhoff; first edition.

7. **Irwin, G. R., (1956)**, "Analysis of Stresses and Strains Near the End of a Crack Transversing a Plate", Journal of Applied Mechanics 24, 361-364.

8. **Song, O., Ha, T., Liberscu, L., (2003)**, "Dynamics of Anisotropic Composite Cantilever Weakened by Multiple Transverse Open Cracks", Engineering Fracture Mechanics 70, 105-123

9. **Przemieniecki, J. S., (1967)**, Theory of Matrix Structural Analysis. London: McGraw-Hill; first edition

10. **Vinson, J. R., and Chou, T. W., (1975)**, Composite Materials and Their Use in Structures. London: Halsted Press/John Wiley; first edition.

11. **Vinson, J. R., and Sierkaowski, R. L., (1991),** Behavior of Structures Composed of Composite Materials, Dordrecht: Martinus Nijhoff; first edition.

12. **Suo, Z., (1990)**, "Delamination Specimens for Orthotropic Materials", Journal of Applied Mechanics 57, 627-634.